SiF 2024 – The 13th International Conference on Structures in Fire
University of Coimbra, Portugal, 19 to 21 June 2024

THERMO-MECHANICAL ANALYSIS AND VALIDATION OF SAFIR FOR HISTORIC FORMS OF CONSTRUCTION

Octavian Lalu[1], Tom Lennon[2], Diana Duma[3], Thomas Gernay[4]

ABSTRACT

This paper presents a comprehensive investigation into the thermo-mechanical analysis and validation of advanced numerical techniques for assessing the fire performance of historic forms of construction. The primary focus is on filler joist floors and hollow pot floors, two significant historical floor types commonly found in structures in the UK dating from the 19th and early 20th centuries.

Keywords: Historic forms of construction, thermo-mechanical analysis, standard fire exposure, SAFIR

1 INTRODUCTION

The main objective of structures-in-fire (SiF) analysis is to determine the thermo-mechanical behaviour of a structure during a fire until failure. The software SAFIR was developed to allow numerical modelling of the behaviour of structures subjected to fire [1]. The software enables thermal analysis, and the information obtained on the temperature distribution can be used to estimate the load-bearing capacity of the members.

For existing historical forms of construction undergoing refurbishment or change of use, it is often necessary to determine the fire resistance of the structural components. The standard fire resistance procedures involve testing individual elements such as columns, beams and floors [2]. Historic buildings often exhibit structural characteristics distinct from modern construction, posing challenges for traditional fire testing approaches [3]. Computational methods may provide an appropriate means to demonstrate compliance with the mandatory requirements of the Building Regulations. The Eurocodes governing structural fire engineering design highlight the need to validate advanced numerical models using relevant experimental data [4,5].

The advanced finite element software SAFIR has been extensively validated and benchmarked against the cases set out in the German National Annex for EN 1991-1-2 (2010) [6-11]. The existing validation studies focus on recent forms of construction and are not necessarily relevant to historic structures.

This paper explores the use of advanced numerical techniques to estimate the anticipated fire behaviour of existing floor systems used in historic buildings in the UK. The main objective is to benchmark the numerical model against standard fire resistance test data for historic floor constructions.

2 METHODOLOGY

The methodology involves using SAFIR software to validate the thermo-mechanical behaviour of historic types of floors using standard fire resistance test evidence.

[1] Senior Fire Engineer, Building Research Establishement,
e-mail:octavian.lalu@bregroup.com, ORCID: https://orcid.org/0000-0003-0461-6526
[2] Principal Fire Engineer, Building Research Establishement,
e-mail:tom.lennon@bregroup.com, ORCID: https://orcid.org/0000- 0002-2786-0591
[3] Senior Fire Engineer, Building Research Establishement,
e-mail:diana.duma@bregroup.com, ORCID: https://orcid.org/0000- 0002-6121-3099
[4] Assistant Professor, Johns Hopkins University
e-mail:tgernay@jhu.edu, ORCID: https://orcid.org/0000- 0002-3511-9226

The numerical analysis is based on two steps. In the first step, a heat transfer analysis is performed to determine the heat distribution through the floor section. The heat transfer by conduction is based on the Fourier Law (equation 1). [1].

The Fourier equation is expressed in equation 1.

$$\frac{\partial}{\partial x}\left(k\frac{\partial T}{\partial x}\right)+\frac{\partial}{\partial y}\left(k\frac{\partial T}{\partial y}\right)+\frac{\partial}{\partial z}\left(k\frac{\partial T}{\partial z}\right)+Q=c_p\rho\frac{\partial T}{\partial t} \quad (1)$$

Where $k_{(\theta)}$ is the thermal conductivity (W/mK), $c_{p(\theta)}$ is the specific heat (J/kgK), $\rho_{(\theta)}$ is the density (kg/m^3), and Q is the internal heat generation (W/m^3). The thermal properties are temperature-dependent.

In the second step, the mechanical analysis is performed based on the temperature output from the thermal analysis, which considers a reduction of the material properties at elevated temperatures. The mechanical problem can be solved in a quasi-static manner using equation 2 or a dynamic formulation.

$$\Delta F = K \cdot \Delta u \quad (2)$$

Where K is the structure's stiffness matrix, ΔF is the vector of incremental applied nodal forces, and Δu is the vector of incremental nodal displacements.

3 PERFORMANCE OF FILLER JOIST FLOORS IN FIRE

Filler joist floor systems are a typical form of construction used in the 19th century. The term *"filler joist"* is a generic one used for certain types of building floors dating from the late Victorian era to World War II. The floors comprise metal beams completely embedded in concrete. The floors can have wrought iron sections or even cast-iron tees in the early period. Usually, they span one way between the supports, and they are encased in concrete made with coke-breeze, clinker, broken brick, or conventional aggregates [12]. The concrete provides mainly insulation for the steel joists. The joists act as the main load-bearing members and are usually spaced at a centre distance ranging from 600mm to 900mm. The joists can rest either on solid masonry walls or on steel beams. The typical overall depth can range from 100m to 300mm based on the steel joist size. General sections through proprietary historic floor systems are shown in Figure 1 [13].

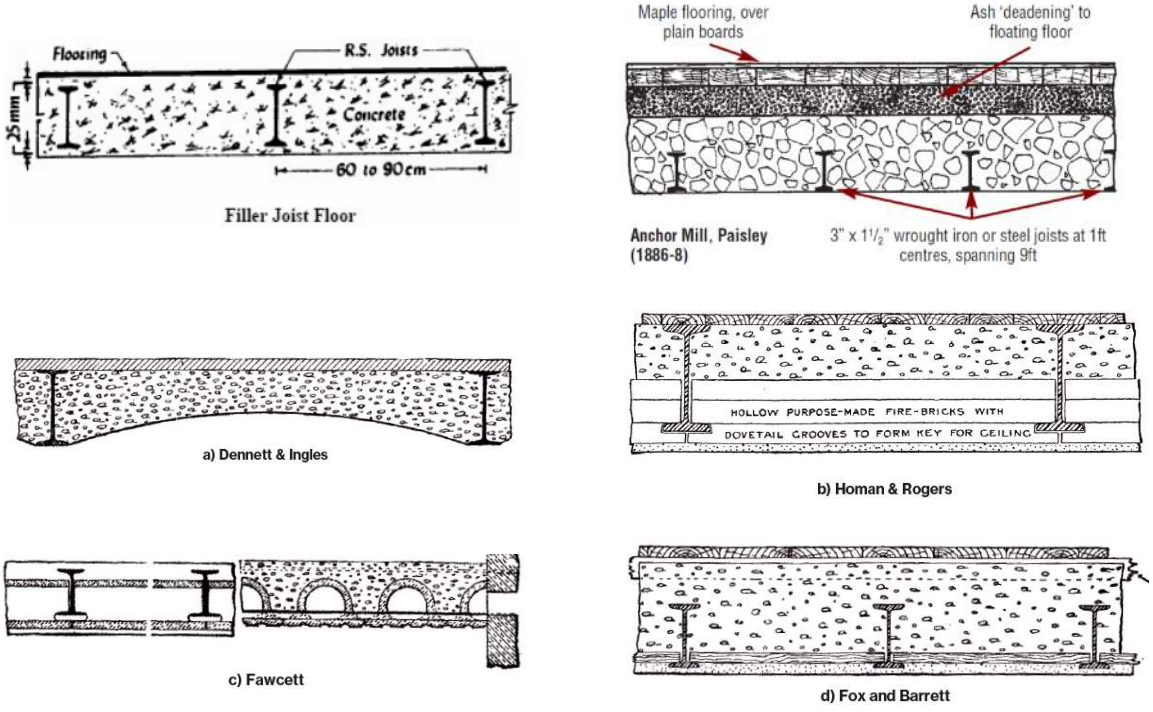

Figure 1. Typical section through a filler joist floor

The concrete cover governs the fire resistance by reducing the heat transfer to the steel section in the event of a fire. The fire resistance of the structure can be compromised if the cover to the joists has been lost by material falling off the soffit. If the soffit cover is missing, it needs to be reinstated. This applies to all filler joist floor systems or jack arches as they have evolved as "fire-proof" solutions [14].

The performance of many innovative floor systems would have been established through fire testing, particularly where reinforced concrete was used alongside other materials to provide the required level of performance. It is improbable that the test data were publicly accessible, and often, the details necessary to validate the fire-resistance performance of these systems are no longer accessible. Some information from standard fire tests, including results from a range of in-situ and precast concrete flooring systems, is available in the literature [16-18].

Figure 2 shows a section through the filler joist floor system used in the standard fire testing and the positions of the instruments. Table 1 summarises the historic test data for filler joist floors.

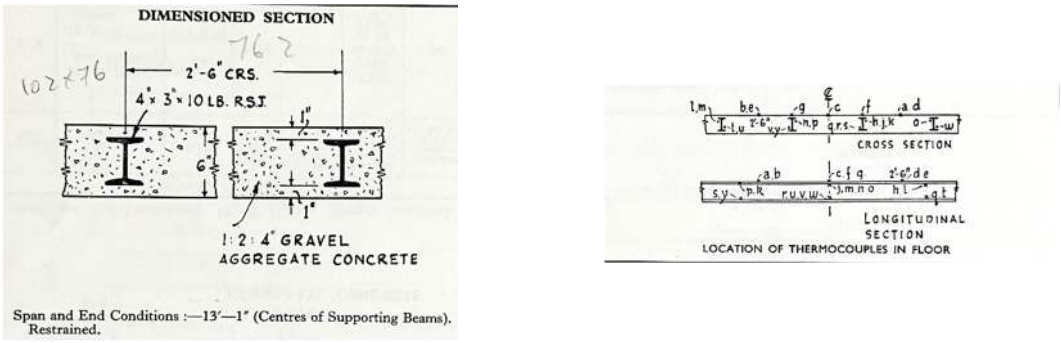

a) General section through the floor system b) Position of the instruments

Figure 2. Section through a filler joist floor subjected to standard fire testing [15]

Table 1 Historic test data for filler joist floors [15]

Test Ref.	Depth of floor (mm)	Joist size (mm)	Cover (mm)	Span (mm)	Test duration (min)	Comments
F30	152	102 × 76	26	762	29	Limited spalling. The test was continued for 180 min. Local integrity failure.
FR1	152	102 × 76	26	762	228	Spalling after 5 min up to 20 min
F62	178	102 × 76	38	762	360	-
F8	184	102 × 76	20	762	240	13mm plaster
F9	184	102 × 76	20	762	120	13mm plaster
F10	159	102 × 76	20	914	240	13mm plaster
F11	159	102 × 76	20	914	240	13mm plaster
F12	159	102 × 76	20	914	150	Limited spalling
F28	152	102 × 45	26	610	270	-
F29	152	102 × 45	26	762	215	-

The tested specimens incorporated granite or crushed brick aggregate and clinker concrete inserts. In all cases, the test duration was limited due to either integrity or insulation failure, often initiated through crack formation or localised temperature rise. None of the tests in the table above had a load-bearing capacity (R) failure mode.

4 PERFORMANCE OF HOLLOW POT FLOORS IN FIRE

Hollow clay pots were first used in the early part of the 20th century as a means of constructing fire-proof floors while reducing the dead load of the building. A typical section is shown in Figure 3 [18].

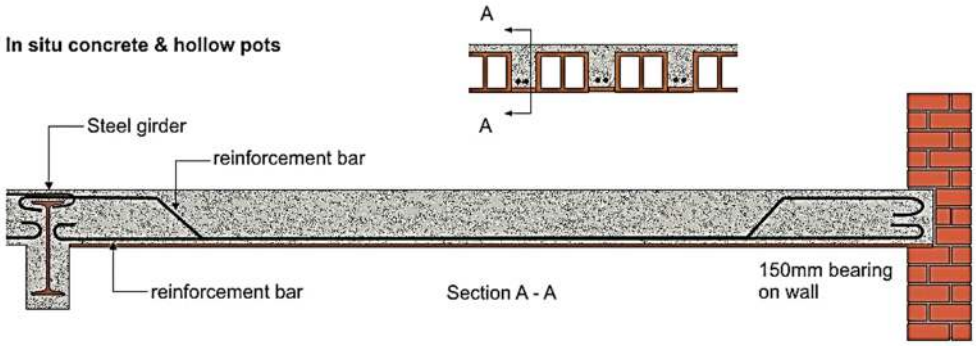

Figure 3. Hollow clay pot floor construction [18]

In general, the hollow pot floor system is one-way, spanning on beams or load-bearing walls. Overall approximate depths vary from 150mm to 300mm with downstand concrete ribs at 400mm-500mm centres. They generally incorporate some form of aesthetic finish to the underside of the soffit (often gypsum plaster) and may have a structural topping or other floor systems on the upper surface. Hollow pot floors are included as a form of plain soffit floor in BS8110-2 [19] and BR128 [20]. However, in many cases, the fire resistance achievable is derived from considering the contribution of the various components to the system, which may well include a plaster finish to the underside of the soffit and any non-combustible structural topping or levelling screed. The anticipated performance when exposed to fire for an existing structure will depend on several factors, including the presence and nature of any defects, the cover to the reinforcement may be insufficient, or the clay pots may be damaged.

Figure 4 and Table 2 below summarise the principal parameters for a number of hollow clay pot floors tested between 1936 and 1945.

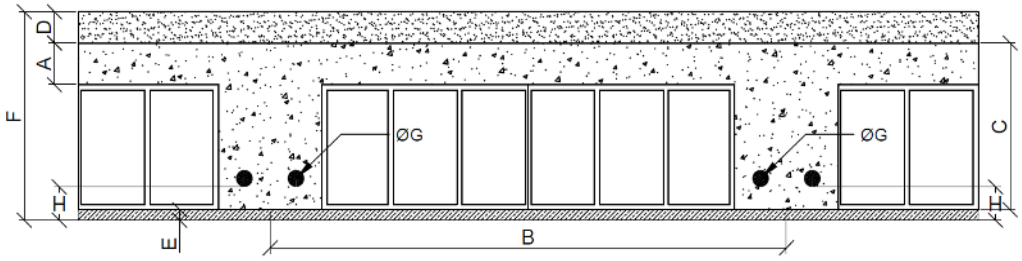

Figure 4. Key components of hollow clay pot floors

A = slab depth; B = span between centre of downstand beams; C = total depth (slab + rib); D = depth of topping; E = thickness of plaster; F = overall depth of construction; G/H= reinforcement specification (diameter + cover)

Table 2. Historic test data for filler joist floor [15]

Test ref.	A	B	C	D	E	F	G/H	Test duration (min)	Mode of failure
F26	38	387	140	0	13	152	2 x 13 @ 19 cover	166	No failure
F27	38	387	140	0	13	152	2 x 13 @19 cover	203	Collapse
F13	38	381	140	73	13	225	1 x 19 @ 19 cover	134	No failure
F14	38	381	140	73	13	225	1 x 19 @ 19 cover	208	Collapse
F15	38	381	140	73	13	225	1 x 19 @ 19 cover	146	Collapse

F32	38	387	140	0	13	152	2 x 13 @ 13 cover	143	Insulation
F59	38	387	140	0	13	152	2 x 13 @ 13 cover	120	No failure
F66	38	387	140	0	13	152	2 x 13 @ 13 cover	120	No failure
F64	38	394	190	0	13	203	2 x 13 @ 25 cover	240	No failure

5 MATERIAL PROPERTIES

Several studies have examined how temperature affects the thermal properties of old concrete. It was found that the thermal properties of concrete, particularly thermal conductivity and specific heat, are influenced by factors such as aggregate type, moisture content, and mix proportions [21-25]. In normal-weight concrete mixes, thermal conductivity typically decreases with increasing temperature until around 700°C, where it stabilises at approximately 0.80–1.20 W/mK. However, the thermal conductivity of lightweight concrete mixes is generally unaffected by temperature variations. This difference is attributed to the increased porosity and voids in lightweight materials, leading to reduced thermal conductivity. The specific heat of concrete was observed to increase between temperatures of 150–400°C due to moisture evaporation, remaining constant beyond that range. These findings highlight the complex relationship between concrete composition and thermal behaviour at elevated temperatures. Figure 5 shows the relationship between various thermal conductivities of concrete and temperature for different types of old concrete and the current and new (λ_{c2022}) Eurocode formulations.

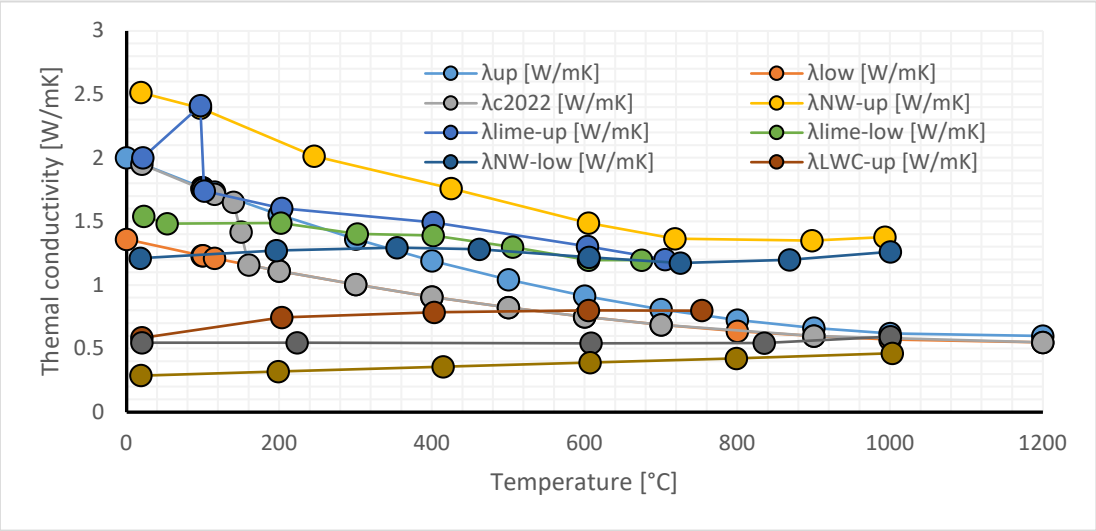

Figure 5. Thermal conductivity for various types of old concrete and the Eurocode formulation

In the early 1800s, cast iron was used as a building material, followed by the introduction of wrought iron. However, after 1850, wrought iron began to be gradually replaced by mild steel, and its usage significantly declined after 1890. Mild steel has many of the properties of wrought iron, with the ultimate tensile and compressive strengths lying roughly between 430-490N/mm^2 [26]. Based on data presented in the literature, deriving precise values for the mechanical and thermal properties of old concrete and steel at elevated temperatures presents a challenge [27,28]. The yield stress reported in the literature for tension reinforcement (plain round or deformed) varies between 230N/mm^2 starting from 1885 to 410N/mm^2 (square twisted) used in the 1960s [29]. However, a thorough comparison with contemporary design codes found that the thermal and mechanical properties of old steel are in good agreement with the expressions provided in Eurocode 3 [5]. The thermal properties of old concrete are similar to those used for modern concrete, as outlined in Eurocode 2 [4].

6 NUMERICAL VALIDATION

6.1 Filler joist floors

In the validation exercise, the boundary conditions from the test evidence are applied to the numerical model. Figure 6 shows the heat transfer through the filler joist floor section and the time-temperature history of the lower and upper flange and the unexposed face.

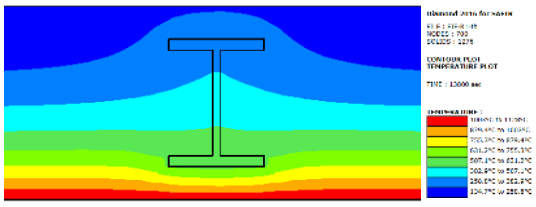

a) Heat distribution through the floor section

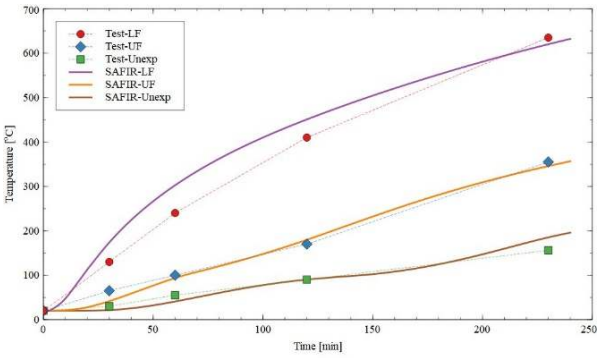

b) Time-temperature of the steel and unexposed face

Figure 6. Heat transfer through the section and the time-temperature history through the section

Figure 7 shows a comparison between the measured temperatures during the ten tests with available data (Table 1) and the calculated values. Deviations of ±15% are indicated on the plot. In the early stages of the fire exposure, there is a slight underprediction or overprediction of the temperature distribution. This can be attributed mainly to steam and moisture migration and other phenomena such as crack formation, spalling and fall-off of the plaster layer. In the latter stages of the fire exposure, the temperature predictions of the structural component are within the expected deviation. In this case, the temperature of interest is above 400°C, where strength reduction factors are applicable to the steel member. The overall accuracy of the numerical heat transfer model fits well in the deviation of ±15%.

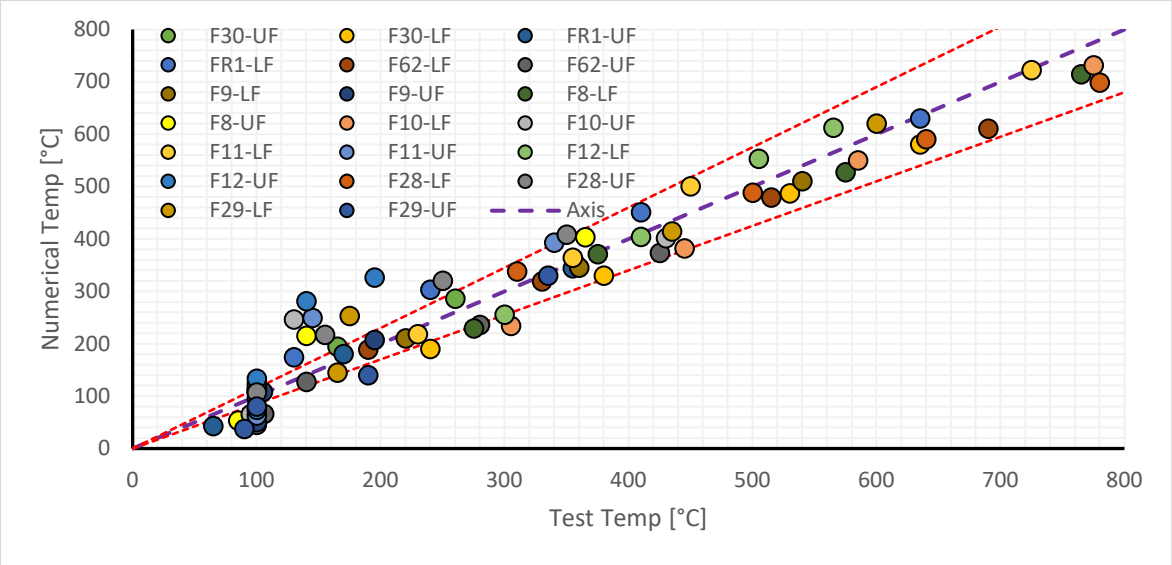

Figure 7. Comparison between calculated and predicted temperatures of the lower and upper flange.

For the structural analysis, the same boundary conditions as those in the standard fire test were applied to the numerical model. The numerical model is simplified to a 2D analysis using beam elements, as shown in Figure 8a. This model assumes a bond between the steel and concrete with a transfer of longitudinal stresses. A summary of the main parameters used in the structural analysis is shown in Table 3 below.

Table 3. Parameters used in the structural analysis for filler joist floors

Test ref.	Density (kg/m^3)	Moisture (%)	Cover (mm)	Conc. Strength (MPa)	Load (kN/m)
F30	2306	5.0	26	26	4.1
FR1	2274	5.2	26	28.8	5.8
F62	2370	7.7	38	28	6.3
F8	2162	4.6	33	22.2	3.5
F9	2242	5.2	33	27.6	3.5
F10	2146	16.1	33	19.3	3.4
F11	1762	10	33	35.3	4.4
F12	1746	8.4	20	24.8	4.4
F28	2259	5.7	26	30.8	1.7
F29	2260	5.9	26	23.8	0.9

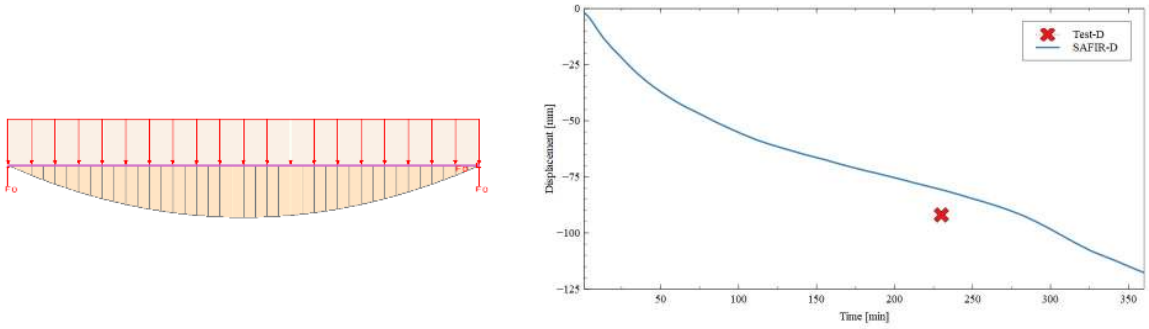

a) General view of the 2D model (FR1)

b) Calculated and measured deflection (FR1)

Figure 8. Model geometry following the test boundary conditions and measured and calculated deflection

Figure 8b shows a comparison between the measured deflection at the end of the test and the calculated deflection for case FR1. During the standard fire test, only one deflection measurement is available. The test was stopped at 228 minutes, and no failure mode was recorded. None of the samples tested presented any load-bearing failure (R) during the standard fire exposure. The expected failure mechanism for filler joist floors would be insulation (I) due to the nonlinear heat transfer through the steel section.

Figure 9 shows the duration of fire exposure for the tested samples and the associated failure mechanisms. The numerical analysis was performed for each tested sample and continued for 240 minutes to identify if there was any potential load-bearing failure mechanism for the samples where the test was stopped. In case F62, the test duration was six hours without any loadbearing failure, also captured in the numerical analysis. For the other samples, the numerical analysis is stopped at 240 minutes because there are no requirements in terms of fire resistance above this value.

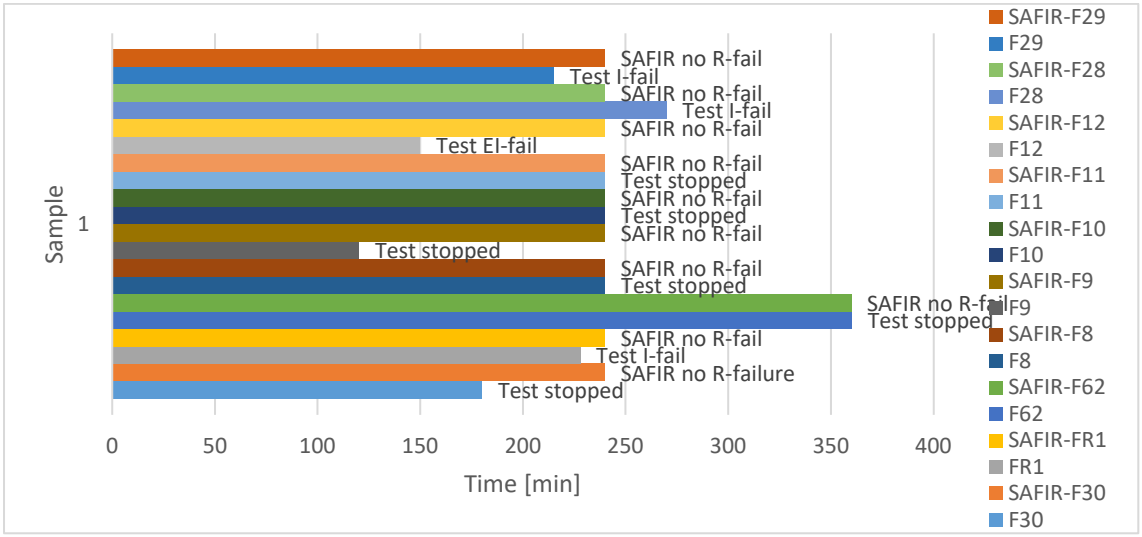

Figure 9. Tested and calculated fire resistance for the filler joist floor samples

6.2 Hollow pot floors

Figure 9 shows the heat transfer through the hollow pot floor section and the measured and calculated time-temperature history of the reinforcement, the upper part of the rib and the unexposed face. A good correlation can be observed between the measured and calculated values.

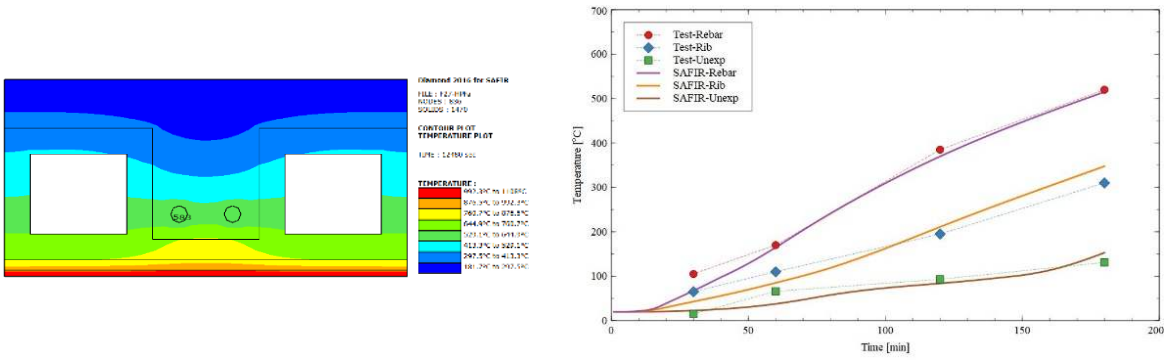

a) Heat distribution through the floor section

b) Time-temperature history of the rebars, the top of the rib and the unexposed face

Figure 9. Heat transfer through the section and the time-temperature history through the section

Figure 10 shows a comparison between the measured temperature of the main reinforcement during the test and the calculated values for the samples with available data and a deviation of ±15%. The overall temperature predictions of the main loadbearing component align with the expected deviation.

For the structural analysis, the same boundary conditions as those in the standard fire test were applied to the numerical model. The numerical model is simplified to a 2D analysis using beam elements, as shown in Figure 11a. A summary of the main parameters used in the structural analysis is shown in Table 4.

Table 4. Parameters used in the structural analysis for hollow pot floors

Test ref.	Density (kg/m^3)	Moisture (%)	Cover (mm)	Conc. Strength (MPa)	Load (kN/m)
F26	2300	5.4	32	42	1.39
F27	2300	5.4	32	41	1.13
F13	2300	5.6	32	30	1.73
F14	2300	5.8	32	25	1.73
F32	2300	5.2	26	53	1.76

F59	2350	5.1	26	44	1.76
F66	2370	4.7	26	45	1.76
F64	2322	5.9	38	30	3.11

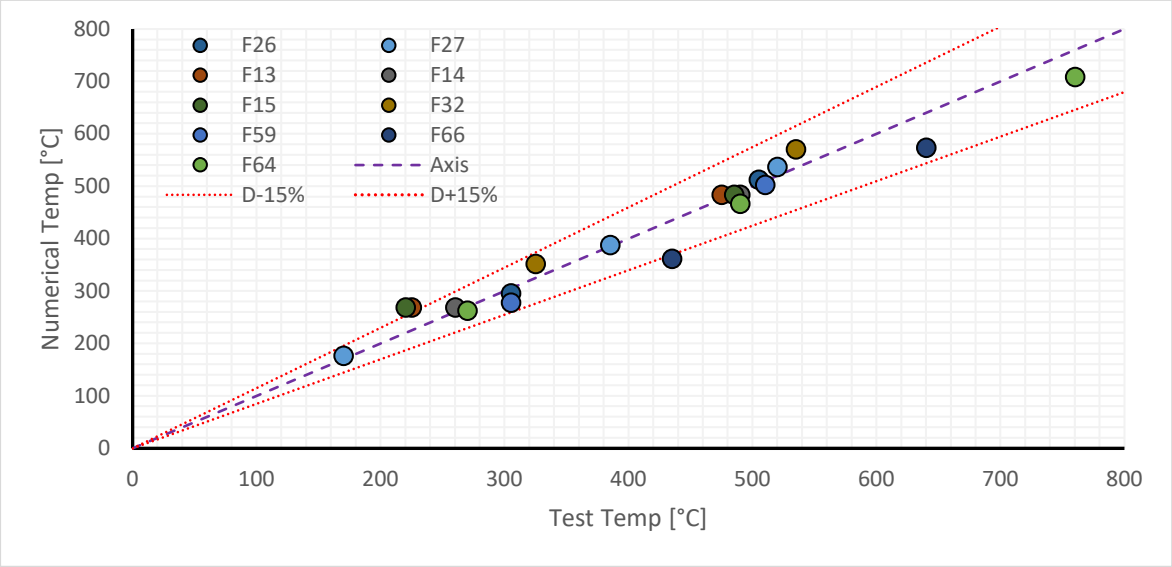

Figure 1 Comparison between calculated and predicted temperatures of the reinforcement layer

Figure 11b shows a comparison between the measured deflection at the end of the tests and the calculated deflection for cases F27 and F14. During the standard fire test, only two deflection measurements were recorded before collapse in the furnace. None of the samples tested presented any load-bearing failure (R) during the standard fire exposure. The expected failure mechanism for filler joist floors would be insulation (I) due to the nonlinear heat transfer through the steel section.

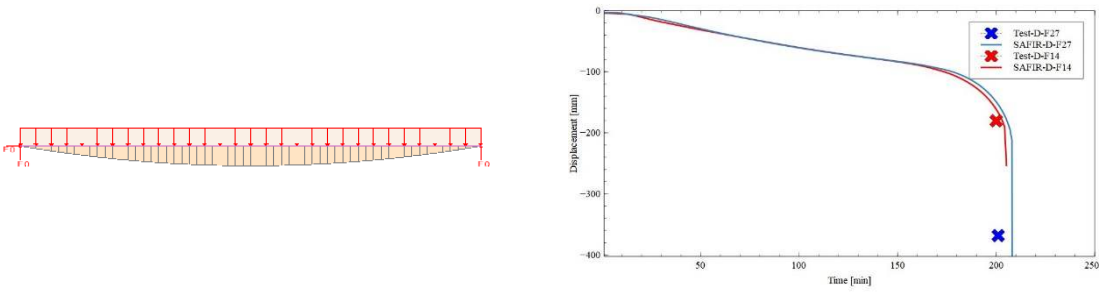

a) General view of the 2D model b) Calculated and measured deflection (F27, F14)

Figure 11. Model geometry following the test boundary conditions and measured and calculated deflection

Figure 12 shows the duration of fire exposure for the tested hollow pot floor samples and the associated failure mechanisms. The numerical analysis was performed for each tested sample and continued to a load-bearing failure for up to 240 minutes. In most cases, the tests were stopped before any failure mechanism occurred. Two tests had a load-bearing failure after three hours of standard fire exposure. The loadbearing failure in these cases was successfully captured within the numerical model with reasonable accuracy, as shown in Figure 11b.

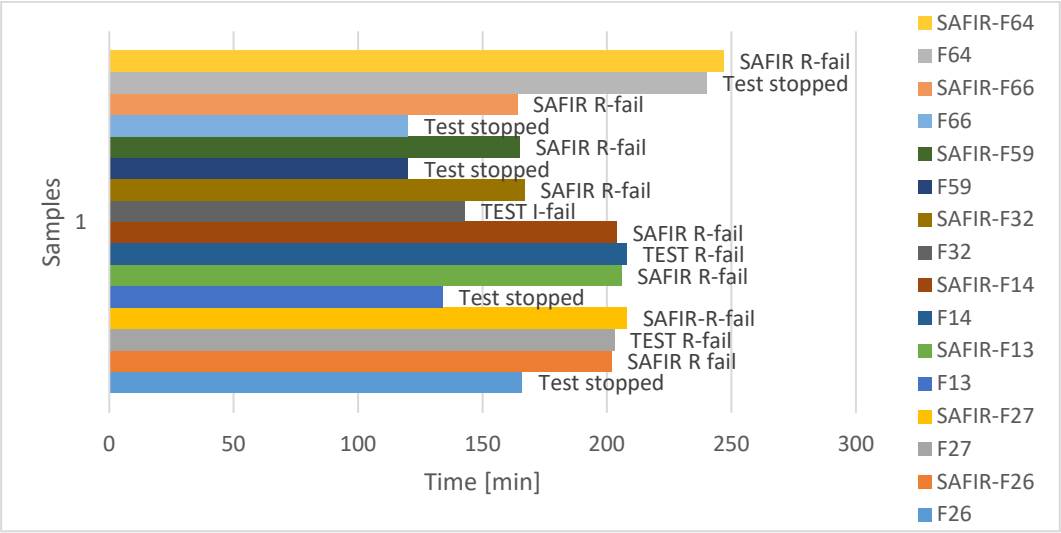

Figure 12. Tested and calculated fire resistance for hollow pot floors

7 DISCUSSIONS AND APPLICABILITY OF THE METHOD

The numerical validation exercise shows the capability of the SAFIR software to capture the thermal distribution through the studied floor systems accurately. The identification of the thermal properties used in the model is essential for its accuracy. The general thermal properties provided by the guidance for concrete, steel, mortar or brick are able to provide accurate results. The analysis found that the lower bound of the concrete thermal properties provides results closer to the measured values from the test.

In some cases, during the early stages of fire exposure, the numerical model overpredicts or underpredicts the temperature distribution. This is because of the complex phenomenon of steam and moisture migration, surface or explosive spalling, crack formation, plaster detachment, etc. These findings align with other studies from the literature [26,27].

The formulation of the concrete thermal properties proposed in the new EN 1992-1-2, which is a combination of the upper and lower bound of the thermal conductivity, is expected to provide more accurate results [30].

The structural analysis of the floor systems was simplified to a 2D model made of beam elements, and the results from the thermal model provided the main input. The loads, material properties and boundary conditions used in the numerical analysis are as close as possible to the samples tested. Where no data was available, assumptions were made based on the literature [27,29]. The stress-stain relationship and associated reduction factors as a function of temperature for the main loadbearing components are based on the formulation from the Eurocodes. The structural analysis performed for the two types of loadbearing floors shows a good correlation between the test data and calculated values.

The expected failure mechanism for the hollow pot floors is the load-bearing capacity (R). There are instances where insulation may be exceeded locally before the loss of capacity, but this is a function of the floor thickness or can be associated with spalling or cracking of the tiles during the fire test.

None of the filler joist floor systems tested presented a load-bearing failure mechanism during the standard fire exposure. Based on the structural analysis, the mechanical behaviour and the floor deflection are captured with a reasonable degree of accuracy.

Insulation failure is the anticipated failure mechanism for the filler joist floors. Loadbearing failure is not a primary failure mechanism because the steel sections encased in concrete have a nonlinear temperature distribution, and the cold side of the section can provide the required level of resistance. The concrete provides insulation and a level of restraint to the steel sections that ensures lateral torsional buckling is not a potential mode of failure of the beams.

Before the analysis, a site investigation must be conducted to identify the nature and extent of any defects. It is also important to determine the condition of the structural elements and if any degradation of materials has occurred over time. For a more detailed overview of the material properties, destructive testing can be performed on concrete cores and steel coupons (samples).

The construction defects can have a significant impact on the anticipated fire resistance of the floor system. The main visible defects for hollow pot floors are cracked or missing tiles or holes through the tiles where ceilings or installations were present (Figure 13a). Another defect can be the shortfall in cover to the reinforcement or segregation in the concrete. It is recommended that a cover survey is conducted and the concrete in the downstand ribs is inspected by removing tiles in relevant areas. For filler joist floors, the main defects are a shortfall in cover to the bottom flange of the steel joists, poor quality of the infill concrete or corrosion of the steel members exposed (Figure 13b). In many cases, the filler joist floors have been designed to be covered with a plaster layer or protected by a lath and plaster ceiling. The defects should be repaired during the refurbishment process. Depending on the nature and extent of the defects, different solutions can be applied.

a) defects present to the underside of a hollow pot floor system

b) defects present to the underside of a filler joist floor system

Figure 13. Examples of defects to the underside of the historic floors considered.

8 CONCLUSIONS

This paper provides a thorough examination of standard fire resistance test data for filler joists and hollow pot floors, which were conducted as part of the Investigation of Building Fires study in the UK during the 1950s. The overarching objective of the paper is to validate the applicability of modern numerical tools such as SAFIR software in evaluating the thermo-mechanical performance of historic forms of construction.

Through the thermo-mechanical analysis and validation exercises, this paper demonstrates the accuracy of advanced numerical techniques in evaluating the fire behaviour of historic forms of construction. Specifically, it aims to validate numerical methods by comparing them against fire resistance test data, focusing on two significant historical floor types: filler joists and hollow pot floors. The analysis presented in the paper shows that the formulation for the material properties (steel, concrete) from the Eurocodes can accurately capture the behaviour in fire of the two floor systems. One limitation is that these numerical methods cannot predict local integrity failure (e.g., cracking or spalling) or the effects of undetected defects.

The study presented in the paper highlights the potential of applying advanced numerical techniques to enhance the understanding and evaluation of the fire performance of historical elements of structure. This not only facilitates more accurate assessments of fire resistance but also offers invaluable insights for architects, engineers, and preservationists involved in the conservation and refurbishment of historic buildings.

REFERENCES

1. Franssen, JM., Gernay, T., Modeling structures in fire with SAFIR®: Theoretical background and capabilities, Journal of Structural Fire Engineering 8, 300-323 (2017). https://doi.org/10.1108/JSFE-07-2016-0010

2. BS EN 13501-2, Fire classification of construction products and building elements, BSI, (2023).
3. Torero, JL., Fire Safety of Historical Buildings: Principles and Methodological Approach, International Journal of Architectural Heritage 13, 926-940, (2019). https://doi.org/10.1080/15583058.2019.1612484
4. BS EN 1992-1-2, Eurocode 2 Design of concrete structures. General rules. Structural fire design, BSI, (2004).
5. BS EN 1993-1-2, Eurocode 3 Design of steel structures. General rules. Structural fire design, BSI, (2005).
6. DIN EN 1991-1-2/NA, National Annex - National determined parameter – Eurocode 1: Actions on structures – Part 1-2: General actions – Actions on structures exposed to fire, Deutsche Norm, (2010).
7. COSTActionTU0904 Integrated Fire Engineering and Response, Case Studies, Ed. Wald F., Burgess I., Rein G., Kwasniewski L., Vila Real P., Horová K. CTU Publishing Production, Czech Technical University in Prague, (2012). ISBN–9788001050040
8. Ferreira, J., Franssen, JM., Gernay, T., Gamba, A., Validation of SAFIR® through DIN EN 1992-1-2 NA Comparison of the results for the examples presented in Annex CC, University of Liege – ArGEnCo – Structural Engineering, (2018).
9. Zaharia, R., Gernay, T., Validation of the advanced calculation model SAFIR through DIN EN 1991-1-2 procedure, International Conference on Advances on Steel Concrete Composite and Hybrid Structures - ASCCS 2012, July 2-4, Singapore, Edited by Liew, JY., and Lee, C.S., ISBN-13: 978-981-07-2615-7, ISBN10: 981-07-2615
10. Ferreira, J.D.R., Gernay, T., Franssen, J.M., Discussion on a systematic approach to validation of software for structures in fire, SiF 2018 The 10th International Conference on Structures in Fire, Fire SERT, Ulster University, Belfast, UK, June 6-8, (2018).
11. Pintea, D., Franssen, J.M., Evaluation of the thermal part of the code SAFIR by comparison with the code TASEF, Proc. 8th Int. Conf. on Steel Structures 2, 636-643, (1997).
12. Miller, J., Conservation compendium. Part 17: Filler-joist floors – development, capacity and typical defects, The Institution of Structural Engineers, (2016).
13. Adams, P., Building Construction, London, UK: Cassells & Co., (1906)
14. Wouters, I., Mollaert, M., Assessing the 19th century 'fire-proof buildings, WIT Transactions on the Built Environment, (2001).
15. National Buildings Studies, Research paper No. 12, Investigations on Building Fires, Part V. Fire tests on structural elements, Her Majesty's Stationary Office, (1953).
16. Fisher, R.W., and Smart, P.M.T., Results of fire-resistance tests on elements of building construction. London, HMSO, Volume 1, (1975).
17. Fisher, R.W., and Smart P.M.T., Results of fire-resistance tests on elements of building construction. London, HMSO, Volume 2, (1977).
18. Lennon, T., Assessing the fire performance of existing reinforced concrete flooring systems, Information paper IP9/12 BRE Press, (2012).
19. BS 8110-2, Structural use of concrete - Part 2: Code of practice for special circumstances, BSI, (1985).
20. BR 128, Guidelines for the construction of fire-resisting structural elements, BRE Press, (1988). Archived
21. Schneider, U., Concrete at high temperatures – a general review. Fire Safety Journal 13, 55–68, (1988).
22. Harmathy, T.Z., Allen, L.W., Thermal properties of selected masonry unit concrete, Am Concr. Inst. Journal 70, 132–42, (1973).
23. Loudon, A.G., The thermal properties of lightweight concrete, Int. Journal of Lightweight Conc. 1, 71–85, (1979).
24. Harmathy, T.Z., Properties of building materials at elevated temperatures, Division of building research, Report no.: 1080, National Research Council of Canada, Ottawa, (1983).
25. Hu, X.F., Lie, T.T., Polomark, G.M., MacLaurin, J.W., Thermal properties of building materials at elevated temperatures, Institute for research in construction, Internal report no.: 643, National Research Council of Canada, Ottawa, (1993).
26. Publication 11/84 Historical structural steelwork handbook, British Constructional Steelwork Association, (1991). ISBN 9780850730159
27. Maraveas, C., Wang, Y.C., Swailes, T., Thermal and mechanical properties of 19th century fire-proof flooring systems at elevated temperatures, Construction and Building Materials 48, 248-264, (2013).doi: 10.1016/j.conbuildmat.2013.06.084
28. Maraveas, C., Wang, Y.C., Swailes, T., Fire resistance of 19th century fire-proof flooring systems: a sensitivity analysis, Construction and Building Materials 55, 69-81, (2014). doi:10.1016/j.conbuildmat.2014.01.022
29. Munter, S., Lume. E., Guide to Historical Reinforcement, CIA Concrete, (2017).
30. Carrascóna. S., Robert, F., Villagrá, C., Some Highlights on the New Version of EN 1992-1-2, (Eurocode 2, Fire part), Hormigón y Acero 74, 223-234, (2023). https://doi.org/10.33586/hya.2023.3096